THE ASTROPHYSICAL JOURNAL, 317:442–449, 1987 June 1

MOLECULES AT EARLY EPOCHS. II. H_2 AND CO TOWARD PHL 957[1]

JOHN H. BLACK
Steward Observatory, University of Arizona
AND
FREDERIC H. CHAFFEE, JR., AND CRAIG B. FOLTZ
Multiple Mirror Telescope Observatory, Smithsonian Institution and the University of Arizona
Received 1986 August 29; accepted 1986 November 18

ABSTRACT

We present 1 Å resolution observations of the spectrum of the QSO PHL 957 obtained with the MMT spectrograph in order to address the question of the existence of molecules at a past epoch. We examine the optically thick metal line absorption system at $z_{abs} = 2.309$ that exhibits a damped Lyman-α line from which a neutral hydrogen column density of $N(H) = 2.5 \times 10^{21}$ cm^{-2} is inferred. We search for absorption features of CO and H_2 without success, and set limits of 2×10^{-8} and 4×10^{-6} for $N(CO)/N(H)$ and $2N(H_2)/N(H)$, respectively, lower than typical Galactic values by factors of 10 and 1.25×10^5.

We use the inferred column densities of the first four stages of ionization of carbon, of H^0 and limits on H_2 to constrain the parameters of photoionization and chemical equilibrium models of the absorbing cloud. We find that the carbon to hydrogen abundance ratio is $\sim 10^{-2}$ of the solar value and that the radiation energy density is nearly 100 times the typical Galactic value. The latter explains the lack of detectable H_2 despite the high neutral hydrogen column density.

We suggest that such an intense radiation field may result from a high rate of star formation in the galactic disk in which the $z = 2.309$ absorption features have been postulated to arise.

Subject headings: interstellar: abundances — interstellar: matter — quasars

I. INTRODUCTION

The existence of molecular absorption toward high-redshift QSOs has been a matter of some controversy. Aaronson, Black, and McKee (1974) presented evidence for molecular hydrogen absorption toward the QSO PHL 957 by identifying five lines at the appropriate wavelengths to be members of the Lyman system at $z = 2.309$. Subsequent data by Coleman *et al.* (1976) increased the number of possible wavelength coincidences to 13. However, the lines of the Lyman and Werner systems, which are expected to dominate the absorption spectrum of H_2 at low temperatures, have rest wavelengths well below that of the Lyman-α line of atomic hydrogen. This places them in the depths of the Lyman-α forest where the absorption spectrum of a high-redshift QSO tends to be sufficiently rich that the identification of any features based solely on wavelength coincidences cannot be considered definitive.

The second most ubiquitous molecule in the universe is likely to be carbon monoxide, whose lines, though much weaker than those of H_2 in Galactic interstellar clouds, for example, lie well longward of H I Lyman-α and therefore are likely to be clear of Lyman-α forest blending toward QSOs.

Recently Levshakov, Khersonskii, and Varshalovich (1986) suggested that a possible absorption feature at 39.3 GHz in a radio spectrum of PHL 61 published by Takahara *et al.* (1984) might be due to the $J = 1$–0 transition of CO (ν_{rest}[vac] = 115.271 GHz) at $z = 1.93$. If this identification is correct, the redshifted lines from the A–X system of CO should be sufficiently strong to be easily detectable in the optical spectrum of PHL 61. Chaffee, Foltz, and Black (1986, hereafter Paper I) searched for these lines and presented upper limits to their strength which suggest that the possible feature at 39.3 GHz cannot arise from CO. Furthermore, they detected no strong Lyman-α absorption at $z = 1.93$ toward PHL 61, absorption which should be evident in a cloud of sufficient column density to produce CO.

Detection of molecules at early epochs would provide a strong diagnostic for the conditions in the clouds that harbor them, and the most promising clouds in which to conduct such a search are those of sufficiently high column density to produce strong Lyman-α absorption. Wolfe *et al.* (1986, hereafter WTSC) present evidence for the existence of a class of "Lyman-α disk systems" toward QSOs in which strongly damped Lyman-α absorption is present and in which even corresponding 21 cm absorption can be occasionally detected. Among the strongest Lyman-α absorbers in the WTSC sample is the high column density cloud at $z = 2.309$ toward PHL 957, and thus it remains the most promising case in which molecular absorption might be detected. Coleman *et al.* (1976) inferred a neutral hydrogen column density, $N(H)$, of $\sim 8 \times 10^{20}$ cm^{-2} and WTSC 2×10^{21} cm^{-2}. A Galactic interstellar cloud of such high H I column density would produce easily detectable H_2 and CO absorption, and we present below observations aimed at their detection.

II. OBSERVATIONS AND REDUCTIONS

Spectroscopic observations of PHL 957 were obtained with the Multiple Mirror Telescope (MMT) and MMT spectrograph during the fall of 1985 using the 832 g mm^{-1} grating blazed at 4000 Å in second order. As summarized in Table 1, the data were recorded in several windows to provide continuous spectral coverage in the range $3150 \leq \lambda \leq 5600$ Å at a resolution of 1 Å (FWHM). The data were reduced as

[1] Observations presented here were obtained with the Multiple Mirror Telescope, a facility operated jointly by the Smithsonian Institution and the University of Arizona.

TABLE 1

PHL 957—JOURNAL OF OBSERVATIONS

Date (UT)	Wavelength Range (Å)	Integration Time (s)
1985 Oct 19	4700–5600	15140
	3800–4700	4800
1985 Nov 9.....	3150–4050	4800
1985 Nov 16	3150–4050	7200
Total.....		31940

described in Paper I, and Figure 1 presents the spectrum of PHL 957 where the wavelengths are vacuum heliocentric, and the 1 σ noise level is shown at the bottom.

a) Metal Species

Table 2 lists all unblended lines from the $z = 2.309$ system with equivalent widths at least 4 times the equivalent width detection limit derived from the measured noise spectrum in Figure 1. The equivalent widths and wavelengths listed in Table 2 (vacuum, heliocentric wavelengths are given throughout this paper) were determined by a software routine which generates an instrumentally broadened Voigt profile and minimizes the χ^2 of the deviations between it and the observed profile by adjusting the position, width, and depth of the line. In order to search for molecular hydrogen absorption line coincidences in the Lyman-α forest, it is essential to have as precise an estimate as possible of the absorption redshift of the

TABLE 2

METAL LINES AT $z = 2.30935$ TOWARD PHL 957

λ_{obs}[a] (Å)	Identification	λ_{rest} (Å)	W_{obs}[b] (Å)	f	N[b, c] (cm^{-2})
3233.32.....	C III	977.026	≤1.2	0.674	≤2.5(15)
3492.32.....	Fe II	1055.269	≤0.16	0.008	≤1.6(15)
3518.31.....	Fe II	1063.180	0.67	0.060	7.2(14)
3580.15.....	Fe II	1081.880	0.47:	0.014	1.5(15):
3629.79.....	Fe II	1096.886	0.70	0.032	1.3(15)
3661.42.....	Fe II	1106.362	≤0.12	0.0015	≤5.9(15)
3712.62.....	Fe II	1121.987	0.46	0.051	3.7(14)
3714.57.....	Fe III	1122.526	0.23	0.050	1.5(14)
3724.11.....	Fe II	1125.450	0.51	0.011	3.2(15)
3789.19.....	Fe II	1144.946	0.76	0.127	2.8(14)
3939.52.....	Si II	1190.416	1.13	0.487	3.0(14)
3949.01.....	Si II	1193.289	1.60	0.874	3.5(15)
4171.52.....	Si II	1260.421	1.48	1.122	6.5(14)
4309.10.....	O I	1302.168	1.69	0.049	4.2(16)
4416.56.....	C II	1334.530	1.60	0.118	7.7(15)
4420.39.....	C II*	1335.703	0.37	0.118	7.6(13)
4612.49.....	Si IV	1393.755	0.25	0.528	9.8(12)
4642.66.....	Si IV	1402.770	0.14	0.262	1.0(13)
5052.66.....	Si II	1526.709	1.32	0.076	1.1(15)
5123.91.....	C IV	1548.188	0.25	0.194	2.1(13)
5132.41.....	C IV	1550.762	0.13	0.097	2.0(13)
5163.72.....	C I	1560.310	≤0.12	0.081	≤2.3(13)
5322.78.....	Fe II	1608.456	1.06	0.062	5.1(14)
5483.47.....	C I	1656.928	≤0.16	0.135	≤1.6(13)
5529.12.....	Al II	1670.787	1.28	1.880	2.3(13)

[a] Wavelengths are vacuum, heliocentric.
[b] Limits are 4 σ.
[c] Estimated by adopting $b = 25$ km s^{-1}.

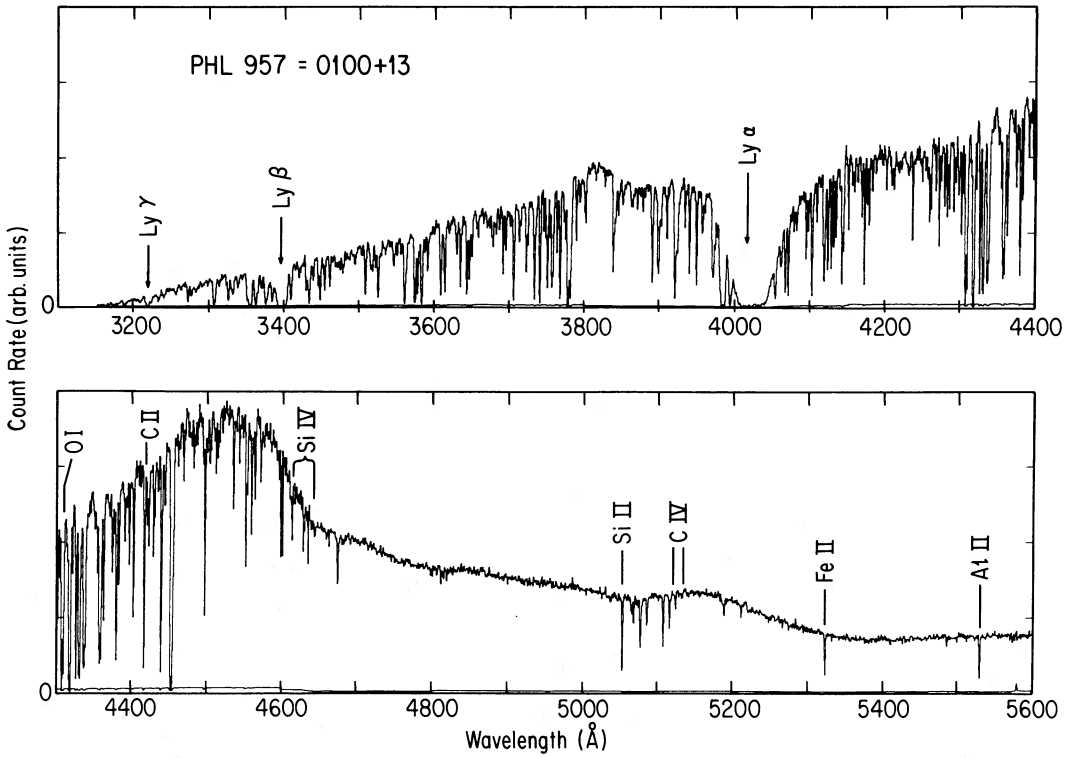

FIG. 1.—1 Å resolution spectrum of PHL 957 obtained with the MMT spectrograph. No attempt has been made to flux calibrate the data so the overall shape of the continuum reflects the wavelength dependent sensitivity of the instrument and atmospheric extinction. The lower curve presents the 1 σ level as derived from count statistics in the object and night sky spectra (plus dark emission). Discontinuities in the error spectrum indicate the edges of individual observations. Absorption lines longward of the Lyman-α forest in the $z = 2.309$ system are marked.

system. To this end we adopt the mean value of $z_{abs} = 2.30935 \pm 0.00024$ inferred from all identified metal lines in Table 2.

The detection of neutral carbon would be of particular interest since its ground term fine-structure levels would be significantly populated by the microwave background at $z = 2$, and the relative strengths of the lines would serve as a sensitive probe of the temperature at that epoch. Neutral carbon is not detected toward PHL 957, and the 4 σ limits on the strengths of $\lambda\lambda$1560, 1656 are listed in Table 2. However, Meyer *et al.* (1986) report its detection toward MC 1331+170 and discuss its implications. They also quote the somewhat smaller upper limit on the neutral carbon column density in the $z = 2.309$ system toward PHL 957 of $N(C) < 4.5 \times 10^{12}$ cm^{-2} (2 σ), which we adopt in the following discussion.

Our resolution is insufficient to resolve the profiles of the lines listed in Table 2, but we have observed several lines of both Fe II and Si II from which a curve of growth can be constructed. This curve of growth provides a "universal" value of 25 km s^{-1} for the Doppler parameter which we then use together with the equivalent width of each line in Table 2 to infer the quoted column densities. Different column densities for lines of the same ion reflect the scatter about the mean curve of growth.

The column densities listed in Table 2 should be regarded as strictly lower limits in view of the possibility that there is unresolved velocity structure in the observed lines. Lacking better information on the line profiles, we will take the column densities at face value in what follows.

b) *Atomic and Molecular Hydrogen*

In order to predict the likely strength of H_2 absorption at $z = 2.309$ we must determine the value of N(H). Figure 2 displays the region near Lyman-α in which we have rectified the data in Figure 1 by eye. We have overplotted three instrumentally broadened Voigt profiles, for $N(H)/10^{21} = 1.25$, 2.5, and 3.75 cm^{-2}, each computed for a Doppler parameter of 25 km s^{-1}. As is the case with all damped lines, the computed profile is very sensitive to the assumed value of N(H). Systematic errors are introduced by uncertainties in the adopted continuum fit, but PHL 957 is relatively uncomplicated in this regard, and our best estimate from Figure 2 of $N(H) = 2.5 \times 10^{21}$ cm^{-2} is in excellent agreement with the value deduced by WTSC. We further estimate that $\lambda_{obs}(Ly\alpha) = 4023.2 \pm 0.2$ Å, in excellent agreement with the predicted wavelength of 4023.08 Å based on the adopted z for the metal lines. Figure 3*a* displays the rectified data between 3200 Å and 3700 Å below which we have plotted the S/N estimate from the photon statistics. We have adopted the parameters from the best fit of Lyman-α to generate the overlaid Voigt profiles for Lyman-β and Lyman-γ. Though difficult to quantify, the match of these profiles to the data lends strong support to our adopted values of z_{abs}, b, and N(H).

In order to estimate better the amount of H_2 toward PHL 957, we have computed synthetic spectra which include Lyman-β and Lyman = γ [computed with $N(H) = 2.5 \times 10^{21}$ cm^{-2} and $b = 25$ km s^{-1}] and 228 lines of the H_2 Lyman and Werner systems for a range of values of $N(H_2)$ and T_{ex}. All lines of H_2 with rest wavelengths $970 < \lambda < 1140$ Å that arise in ground-state rotational levels $J \leq 7$ are included in the simulations.

WTSC have suggested that damped Lyman-α absorption such as that seen toward PHL 957 arises in galactic disks penetrated by our line of sight. The physical conditions in such disks may be similar to those in Galactic interstellar clouds, and we begin by comparing the molecular hydrogen fraction, $f\{= 2N(H_2)/[N(H + H^+ + 2H_2]\}$ in the $z = 2.309$ cloud to that in the Galaxy.

The value of f in single Galactic clouds of such high N(H) usually lies in the range $0.05 \leq f \leq 0.50$, and such clouds typically have an excitation temperature of $T_{ex} \approx 100$ K (Spitzer

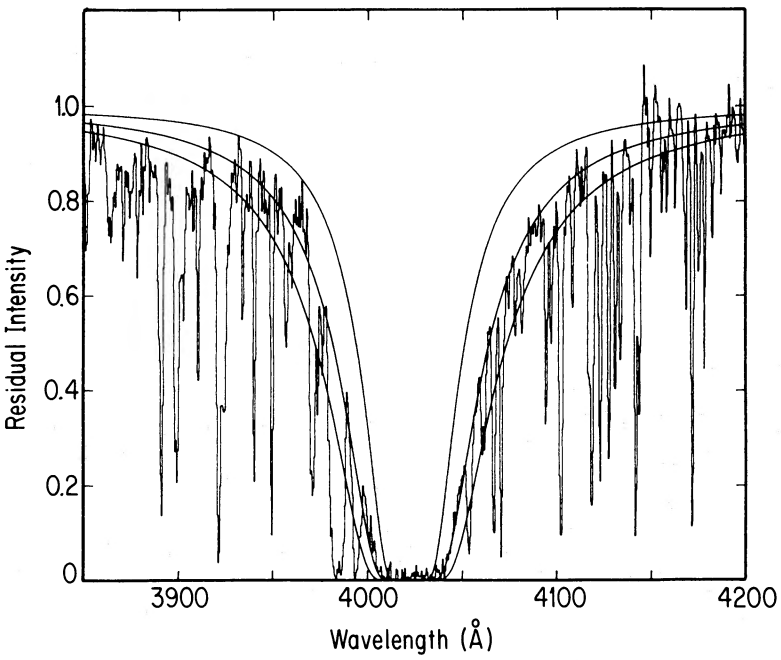

FIG. 2.—Result of Voigt profile fitting to the damped Lyman-α absorption at $z = 2.30935$. The adopted b value was 25 km s^{-1}. The three model profiles are for H I column densities of 1.25×10^{21}, 2.5×10^{21}, and 3.75×10^{21} cm^{-2}.

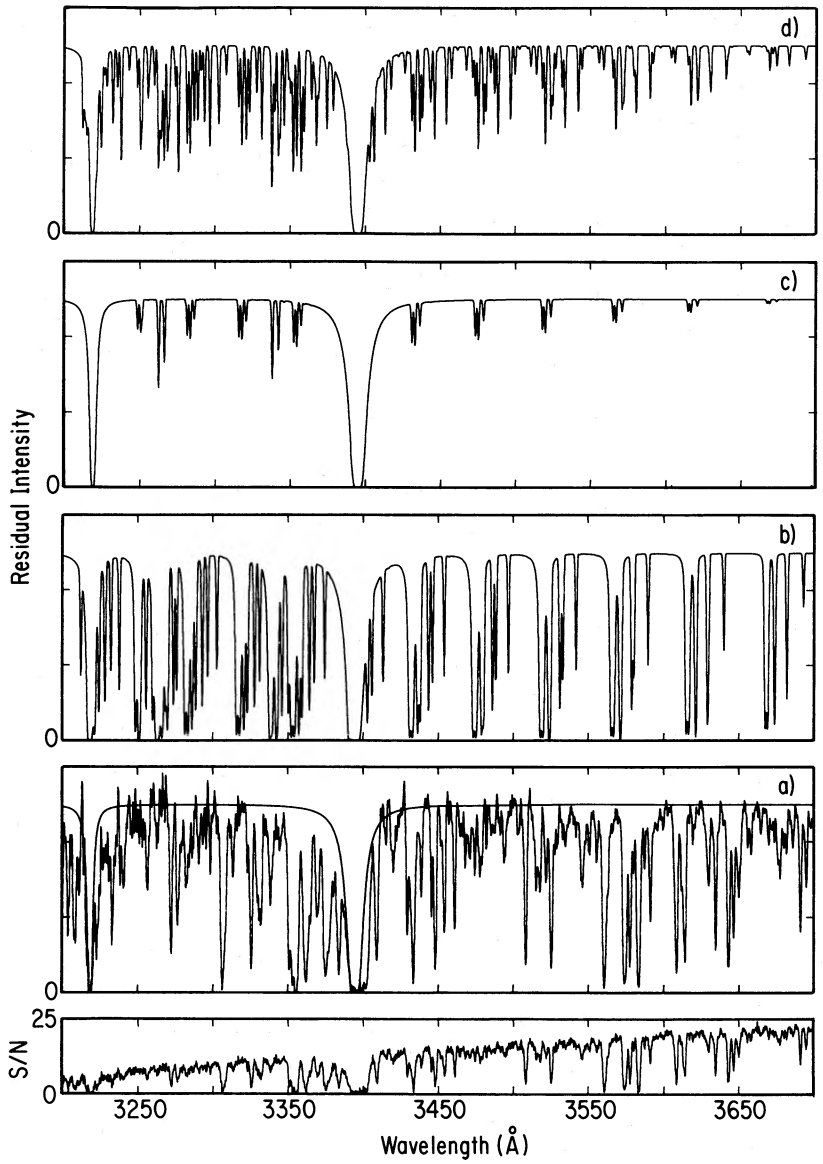

FIG. 3.—(*a*) Fits to Lyman-β and Lyman-γ using the parameters derived by profile fitting of Lyman-α: $z = 2.30935$, $b = 25$ km s^{-1}, and $N(H) = 2.5 \times 10^{21}$ cm^{-2}. The measured signal-to-noise ratio of the data is plotted at the bottom. (*b*) A synthetic spectrum for $N(H_2) = 6 \times 10^{19}$ cm^{-2} at $T_{ex} = 100$ K. (*c*) A synthetic spectrum for $N(H_2) = 10^{15}$ cm^{-2} at $T_{ex} = 100$ K. The strongest predicted features arise from the 0–0 and 1–0 bands of the Werner system. (*d*) A synthetic spectrum for $N(H_2) = 10^{16}$ cm^{-2} and $T_{ex} = 1000$ K. Figs. 3*b*–3*d* include Lyman-β and Lyman-γ having the parameters given for Fig. 3*a*.

and Jenkins 1975). Thus we would expect an H_2 column density of at least $\sim 6 \times 10^{19}$ cm^{-2} for a predominantly neutral Galactic cloud having the same N(H) as that at $z = 2.309$ toward PHL 957.

We have used these values to generate the synthetic spectrum presented in Figure 3*b*, and it is clear that the molecular hydrogen lines would dominate the spectrum of PHL 957. No evidence for such a high H_2 column density is seen in Figure 3*a*. In fact, the lack of detectable features in the small continuum "windows" where the (0, 0) and (1, 0) bands of the Werner system are expected, excludes any values of $N(H_2)$ in excess of 10^{15} cm^{-2} at $T_{ex} \approx 100$ K, as shown in Figure 3*c*. This implies $f < 10^{-6}$ at $T_{ex} \approx 100$ K.

In the Galaxy, such a low value of the molecular hydrogen fraction is observed only in clouds of much lower N(H) where T_{ex} is found to be as high as 1000 K (see, e.g., Morton and Dinerstein 1976). Such a temperature may therefore be more appropriate for the $z = 2.309$ cloud toward PHL 957. At $T = 1000$ K the H_2 will be distributed among many levels, creating a "molecular hydrogen forest" as shown in Figure 3*d* where we have adopted $N(H_2) = 10^{16}$ cm^{-2}.

It is easy to understand from detailed comparison of the panels in Figure 3 why previous investigators have found many coincidences between the predicted locations of H_2 lines and absorption features in QSO spectra. The present work suggests that a less ambiguous test of the existence of H_2 is the *anticoincidence* of predicted H_2 features with the observations. Since high excitation temperatures are likely in regions of low molecular hydrogen fraction, we have adopted $T = 1000$ K in an effort to set the most realistic (and conservative) upper limit to the value of $N(H_2)$ in the cloud toward PHL 957.

In the top panel of Figure 4 we present the data for

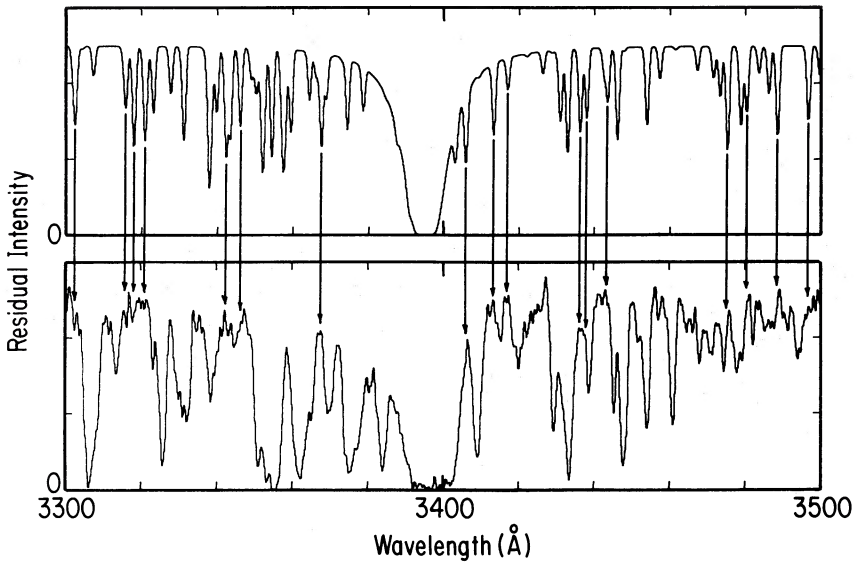

FIG. 4.—(*top*) Expanded view of Fig. 3*a* over the range $3300 \leq \lambda \leq 3500$ Å. (*bottom*) Expanded view of Fig. 3*d*. Anticoincidences between the observed spectrum and the synthetic H_2 spectrum are marked.

PHL 957 in the region in which the largest number of prominent anticoincidences occur. The bottom panel of Figure 4 presents the synthetic H_2 spectrum for $T_{ex} = 1000$ and $N(H_2) = 10^{16}$ cm^{-2} on which we have marked 17 clear anticoincidences. Velocity displacements of order 15 km s^{-1} are found between atomic and molecular species in Galactic clouds (York 1975), and if this value holds at $z = 2.309$, it is much too small to alter significantly the number of observed anticoincidences. From Figure 4 and other syntheses at lower $N(H_2)$ we estimate that if $N(H_2)$ exceeds 5×10^{15} cm^{-2} toward PHL 957, its presence would have been revealed by our data. We therefore adopt this value as a fairly conservative upper limit in the discussion that follows.

c) *Carbon Monoxide*

The rest wavelengths of the dominant lines of the A–X system of CO lie sufficiently longward of Lyman-α to be free from Lyman-α forest blending in PHL 957, and we have searched for the (0, 0)–(4, 0) bands in our data. Table 3 summarizes these results where we have again adopted $b = 25$ km s^{-1} to infer the upper limits to the column density given in the sixth column. From these limits we see that $N(CO)/N(H + 2H_2) \leq 2 \times 10^{-8}$, a value at least an order of magnitude lower than that found in diffuse (Morton 1975; Wannier, Penzias, and Jenkins 1982) or thick molecular (Black and Willner 1984) clouds in the Galaxy.

TABLE 3

CO UPPER LIMITS AT $z = 2.30935$ TOWARD PHL 957

Band	λ[a] (Å)	f[b]	λ (Å)	W_{obs}[c] (Å)	N[d] ($\times 10^{13}$ cm^{-2})
0, 0.....	1544.39	0.0156	5110.93	≤0.10	≤9.7
1, 0.....	1509.70	0.0343	4996.13	≤0.10	≤4.5
2, 0.....	1477.52	0.0411	4889.63	≤0.10	≤4.1
3, 0.....	1447.31	0.0360	4789.66	≤0.10	≤4.8
4, 0.....	1419.00	0.0257	4695.97	≤0.10	≤6.9

[a] Wavelengths are vacuum, heliocentric.
[b] Oscillator strengths are based on the transition moment for CO by Field *et al.* 1983.
[c] Limits are 4 σ.
[d] Estimated by adopting $b = 25$ km s^{-1}.

III. DISCUSSION

As noted above, the molecular hydrogen abundance at $z = 2.309$ toward PHL 957 is low compared with that expected for a single Galactic cloud of comparable column density of neutral, atomic hydrogen. A quantitative analysis of absorption line data such as those presented in Table 2 can yield more detailed information about how dilute matter at earlier epochs differed from the current interstellar medium in the Milky Way.

For the purposes of discussion, the absorbing gas at $z = 2.309$ is taken to be a single, uniform cloud of temperature T, total hydrogen density $n_H = n(H) + 2n(H_2) + n(H^+)$, that is exposed to an isotropic power-law radiation field of mean flux

$$\phi_\nu = \frac{4\pi I_\nu}{h_\nu} = 3 \times 10^{-8} \phi_0 \left(\frac{\nu}{10^5 c}\right)^{-\alpha} \text{ photons s}^{-1} \text{ cm}^{-2} \text{ Hz}^{-1}.$$

The scaling factor in ϕ_ν is normalized so that $\phi_0 = 1.0$ corresponds to the mean interstellar radiation field in the local Galactic plane at 1000 Å, viz., $\phi \approx 3 \times 10^{-8}$ s^{-1} cm^{-2} Hz^{-1} (Draine 1978). The Galactic radiation field from the near-infrared through the visible to the hydrogen Lyman limit in the far-ultraviolet is well described by such a simple power law with $\alpha = 2.7$ (van Dishoeck and Black 1982). The abundances and excitation of various atomic and molecular species are assumed to be in steady state. For comparison with observations, ratios of local number densities, $n(X)/n(Y)$ are assumed to scale directly as the corresponding ratios of observed column densities, $N(X)/N(Y)$. Thus the details of radiative transfer and internal structure within the absorbing region have been neglected. Observational data of even higher resolution and higher S/N will probably be needed to compel a more sophisticated modelling effort.

Within this simple framework, the equations of ionization and chemical balance among the principal forms of hydrogen, helium, and carbon (H, H^+, H_2, H^-, H_2^+, H_3^+, He, He^+, He^{+2}, HeH^+, C, C^+, C^{+2}, C^{+3}, C^{+4}, C^{+5}) are solved simulta-

neously with those that govern the excitation of ground-state fine-structure levels in C and C^+. This calculation will eventually be expanded to include nitrogen, oxygen, silicon, and iron, and details will be presented elsewhere. The resulting atomic and molecular concentrations as functions of α, ϕ_0, n_H, and T can be compared with the observations to extract diagnostic information. The principal diagnostic measurements are $N(H_2)/N(H)$, $N(C^+)/N(C)$, $N(C^{+2})/N(H)$, $N(C^{+3})/N(H)$, and $T_{ex}(C^+)$, where

$$T_{ex}(C^+) = 91.25/\ln (2N_{1/2}/N_{3/2}) \text{ K}$$

is the excitation temperature that characterizes the relative populations of the $^2P_{1/2}$ and $^2P_{3/2}$ levels of the ground term of C^+. The best available atomic and molecular data on cross sections for photoionization and photodissociation, rates of radiative recombination, rates of charge transfer, etc., have been used in the calculations. A helium abundance

$$n(\text{He}) + n(\text{He}^+) + n(\text{He}^{+2}) = 0.75 n_H$$

(Yang *et al.* 1979) has been adopted.

The carbon abundance is determined from the measurements of C I, C II, C III, and C IV lines and the consistent analysis that estimates the concentrations of the unseen stages of ionization.

The only rather uncertain microscopic rate is that for the formation of H_2 from H atoms on dust particle surfaces. In the Galactic interstellar medium, this is the main mechanism by which H_2 forms and its efficiency is high provided that the equilibrium grain temperature is relatively low ($T_{dust} \lesssim 20$ K). In the Galactic case then, the H_2 formation rate can be estimated on the basis of a grain cross sectional area inferred from interstellar extinction measurements. There is no independent evidence for any measurable extinction toward PHL 957; hence, the dust abundance may be quite low in the $z = 2.309$ absorption region. The rate of formation of H_2 per H atom striking a dust grain of mean geometrical cross section σ_d can be written

$$n(\text{dust}) v_H(T) \kappa(T_{dust}) = 4.5 \times 10^{-18} n_H T^{1/2} y_f \text{ s}^{-1} ,$$

where $v_H(T)$ is the mean thermal velocity of H atoms at a gas temperature T and κ is the adsorption/formation efficiency. This rate has been parametrized so that the scaling factor $y_f \approx 0.5$–1 in the local Galactic interstellar medium. The rate can be related to the dust abundance A_d as a fraction of the total mass of hydrogen, the mean density of a dust particle ρ_d in grams cm^{-3}, and the cross section σ_d in cm^2

$$y_f = \left[\frac{\kappa(T_{dust})}{0.25}\right]\left(\frac{A_d}{0.01}\right)\left(\frac{1.0}{\rho_d}\right)\left(\frac{\pi \times 10^{-10}}{\sigma_d}\right)^{1/2} .$$

Even if $y_f \approx 0$, H_2 can be formed by the gas phase processes

$$H^- + H \rightarrow H_2 + e$$

and

$$H_2^+ + H \rightarrow H_2 + H^+$$

which have been included in the present calculations along with all major processes that affect the abundances of the intermediate species H^- and H_2^+.

Table 4 lists the observational constraints together with derived properties of several models, four of which satisfy all of the constraints simultaneously. These constraints are taken at face value. This means, for example, that the lines of highly ionized species like C IV are assumed to be formed in the same volume of gas as those of species like H I, C II, and H_2. The C^{+3}/H ratio is particularly useful as a means of placing limits on the fractional ionization of H and He within the absorbing cloud. At a column density, $N(H) = 2.5 \times 10^{21}$ cm^{-2}, the optical depth at cloud center due to continuous absorption by H, $\tau_H = N(H)\sigma_H(\nu)/2$, reaches a value of order unity at $\nu/c = 2.2 \times 10^6$ cm^{-1} or $\lambda = 45$ Å. Therefore it can be assumed that $\phi_\nu \approx 0$ for all wavelengths in the range $45 < \lambda \lesssim 912$ Å.

TABLE 4

PHL 957 CLOUD MODELS

Property	Observed	Model 1	Model 2	Model 3	Model 4	Model 5
α	...	2.0	2.0	2.0	2.0	2.1
[C]/[H]	4.1(−6)	4.1(−6)	4.1(−6)	4.1(−6)	4.1(−6)	4.1(−6)
n_H (cm^{-3})	...	1.2	1.9	5.6	1.2	1.2
T (K)	...	4000.	105.	42.5	4000.	4000.
ϕ_0	...	6.0	10.	30.	6.0	6.0
y_f	...	1.0	1.0	1.0	0.0	1.0
$N(H)$	2.5(21)	2.5(21)	2.5(21)	2.5(21)	2.5(21)	2.5(21)
$n(H^+)/n_H$	...	5.02(−2)	1.29(−2)	9.84(−2)	5.02(−2)	4.19(−2)
N(He)	...	7.1(19)	1.4(20)	1.5(20)	7.1(19)	8.1(19)
$n(He^+)/n$(He)	...	1.58	0.356	0.247	1.58	1.28
$n(He^{+2})/n$(He)	...	2.15(−1)	1.60(−2)	8.74(−3)	2.15(−1)	1.43(−1)
N(C)	<4.5(12)	6.3(11)	1.3(12)	1.8(12)	6.3(11)	5.9(11)
$N(C^+)$	7.8(15)	8.3(15)	7.2(15)	7.5(15)	8.3(15)	8.9(15)
$N(C^{+2})$	≤2.5(15)	2.3(15)	2.0(15)	2.1(15)	2.3(15)	1.7(15)
$N(C^{+3})$	2.0(13)	2.0(13)	1.8(13)	1.9(13)	2.0(13)	1.4(13)
$N(C^{+4})$	...	6.5(13)	1.0(15)	7.2(14)	6.5(13)	3.4(13)
$N(H_2)$	<5.0(15)	2.6(15)	4.1(14)	2.6(14)	3.6(13)	2.6(15)
$n(H^-)/n_H$	...	1.22(−9)	1.89(−11)	5.70(−12)	1.22(−9)	8.80(−10)
$n(H_2^+)/n_H$	...	2.58(−9)	3.09(−9)	2.57(−9)	2.58(−9)	2.46(−9)
$n(H_3^+)/n_H$	...	1.47(−12)	1.43(−12)	1.08(−12)	2.08(−12)	1.61(−12)
$n(HeH^+)/n_H$	...	7.27(−9)	1.78(−8)	1.64(−8)	7.27(−9)	6.82(−9)
$T_{ex}(C^+)$	17.2	17.2	17.2	17.2	17.2	16.8
$n(e)/n_H$	...	1.04(−1)	3.41(−2)	2.57(−2)	1.04(−1)	9.03(−2)
W_λ(10830) (Å)	...	0.0204	0.0619	0.193	0.0204	0.0164

The predominant source of C^{+3} in the current context is K-shell photoionization of C^+ that is accompanied with high probability by the ejection of a second electron through the Auger effect (Weisheit 1974). The threshold for this process is $\nu/c = 2.4 \times 10^6$ cm^{-1} or $\lambda = 42$ Å; therefore, the same part of the ionizing spectrum is effective in producing H^+, He^+, and C^{+3}. We note that the contribution to the cloud optical depth from K-shell absorption by C^+ is of order only 10^{-2} even at the K-shell edge. Contributions from He and He^+ are such that for all models in Table 4, the optical depth drops below unity for all $\lambda \lesssim 33$ Å.

Thus, the C^{+3}/C^+ abundance ratio fixes the ratio of hard to soft photon fluxes (i.e., the value of α) and constrains the abundances of the unseen ions of hydrogen and helium. In regions of relatively low overall ionization, C^{+3} is removed primarily by charge transfer with H and He rather than by recombination with electrons; thus to first order, $n(C^{+3})/n(C^+) \propto \phi_0/n_H$. Because H_2 is formed by processes whose rates per H atom vary approximately as n_H and because it is destroyed mainly by photodissociation, a similar behavior is expected for the molecular abundance: $n(H_2)/n_H \propto \phi_0/n_H$. The behavior of the $n(C^+)/n(C)$ ratio is more complicated owing to the fact that C^+ is formed both by ionization of C and by recombination of C^{+2}. The parameter $T_{ex}(C^+)$ is also a complicated function of T, n_H, and ϕ_0, and will approach $T_{ex}(C^+) \approx T$ only in the limit of very small ϕ_0/n_H. In the limit of large ϕ_0/n_H, $T_{ex}(C^+)$ will approach a value intermediate between that determined by the cosmic background radiation, $T_B \approx 2.7(1 + z)$, and that determined by radiative excitation in the ultraviolet transitions of C II.

The results of models 1 through 3 in Table 4 show that the observations can be reproduced well by a range of parameters. Models with densities outside the range $n_H \approx 1$–6 cm^{-3} and temperatures outside the range $T \approx 40$–5000 K violate one or another of the observational constraints. The ratio of photon flux to gas density is well-determined, with $\phi_0/n_H = 5.2 \pm 0.2$ for all allowed models. The fractional ionization is low, $n(e)/n_H \lesssim 0.1$, but not negligible, in all cases. Even with the use of a high formation rate of H_2 ($y_f = 1.0$ in models 1, 2, 3, and 5) the predicted abundance of the molecule is still well below the measured upper limit. This is because $\phi_0/n_H \approx 5$, which is approximately 100 times larger than the typical values in the diffuse interstellar medium of the Milky Way where H_2 is seen (see, e.g., Jura 1975; van Dishoeck and Black 1986). In other words, H_2 is not present in the $z = 2.309$ cloud toward PHL 957 despite conditions of relatively low ionization and a large abundance of neutral H because the flux of ultraviolet photons there is still too high for H_2 to exist in an amount sufficient to shield itself against photodissociation. Model 4 is identical to model 1 except that H_2 is formed by gas phase processes only ($y_f = 0$).

Model 5 illustrates the effect of a change in the slope of the spectrum of the radiation field. The ultraviolet part of the spectrum controls the C^+/C ratio and the H_2 abundance, while the soft X-ray part of the spectrum controls the ionization of H, He, and the higher stages of carbon. The parameter α characterizes the relative intensities of the two ends of the spectrum. It is only in cases such as we are considering here where species of low ionization and high ionization are considered together that the results are sensitive to the value of α. Model solutions are less satisfactory for $\alpha \lesssim 1.9$ and $\alpha \gtrsim 2.2$.

As shown in Table 4, the acceptable models are rather insensitive to temperature. Such model calculations can, however, be used to identify potential diagnostic probes that would constrain T better. One example is the predicted concentration of metastable He in the $2s\ ^3S$ state, which is in principle observable through absorption lines at vacuum rest wavelengths of 10833.135, 3889.745 Å, etc. The rest equivalent widths at $b = 25$ km s^{-1} for the He I 10830 Å line are listed in Table 4. In the relevant part of $\phi_0 - n_H$ parameter space, the concentration of He($2s\ ^3S$) is given simply by the balance of production by recombination of He^+ and of loss by spontaneous magnetic diplole transitions to the ground state:

$$n(2s\ ^3S) = 9.6 \times 10^{-7} T^{-0.7128} n(e) n(He^+) \text{ cm}^{-3} .$$

The lowest temperature model predicts a redshifted He I line at $\lambda = 3.585$ μm that would be detectable in a spectrum with $S/N = 60$ at a resolving power of $\lambda/\Delta\lambda = 1000$.

The carbon abundance implied by the observations of lines of the four lowest stages of ionization is $[C]/[H] = 4.1 \times 10^{-6}$, which is only 0.0088 times the solar abundance (Lambert 1978).

The $z = 2.309$ absorption region is evidently exposed to a high ultraviolet flux, $\phi_0 \approx 6$–30. For comparison, the integrated light of QSOs at $z \approx 2$ probably corresponds to $\phi_0 \lesssim 0.1$ and the contribution of PHL 957 itself (at $z_{em} = 2.69$) is $\phi_0 \approx 10^{-5}$, if the difference between emission and absorption redshifts is purely a result of Hubble expansion at $H_0 = 100$ km s^{-1} Mpc^{-1}. One possible explanation of the intense radiation field is that the absorption may arise in a disk galaxy undergoing a burst of massive star formation at $z = 2.3$. Any calculation of the emergent Lyman-α flux from the absorbing cloud is extremely sensitive to details of the cloud geometry and dust properties. It is interesting to note, however, that Foltz, Chaffee, and Weymann (1986) report a marginally significant (2.5 σ) detection of flux in the bottom of the Lyman-α absorption line in the data presented here. This detection implies a surface brightness of the absorber in Lyman-α of $\lesssim 8.2 \times 10^{-17}$ ergs s^{-1} cm^{-2} arcsec^{-2}.

The absence of CO is not surprising in view of the very small abundance of H_2. In the sense that large column densities of H_2 must be present for CO to be self-shielding in Galactic clouds, CO is even more fragile than H_2 in relatively intense ultraviolet radiation fields (van Dishoeck and Black 1986).

IV. SUMMARY

Absorption line observations of the strong Lyman-α disk system at $z = 2.309$ toward PHL 957 combined with theoretical models of the ionization and chemical equilibria in such a cloud have revealed the following:

1. The hydrogen number and column densities in the cloud are similar to those in diffuse Galactic interstellar clouds.
2. The C/H ratio in the cloud is slightly less than 10^{-2} of the solar value.
3. The ratio of photon flux to gas density is approximately 100 times larger and the ionizing spectrum is harder than in typical diffuse interstellar clouds in the Galaxy. One plausible explanation of such a result is that the star formation rate was much higher at earlier epochs.
4. The molecular hydrogen fraction is at least 125,000 times lower than that typical of Galactic interstellar clouds. Even in the presence of dust, on whose surfaces H_2 forms at high efficiency, this limit is not unexpected since photodissociation caused by the high ultraviolet photon flux will suppress the equilibrium abundance of molecuar hydrogen.

5. The observed CO/H value is at least an order of magnitude less than that in the Galaxy.

The above results suggest several topics for further investigation.

1. Because the same photons at $\lambda \approx 1000$ Å are effective in destroying H_2 and in ionizing neutral carbon, the most favorable QSO absorption-line systems to search for molecules are likely to be those that exhibit detectable lines of C I. In such regions, the H_2/H ratio will be useful in placing constraints upon the dust abundance.

2. Clouds of low ionization and high optical depth with even richer absorption spectra can be used to further constrain the physical conditions. In particular, systems revealing C I and O I absorption and having stringent limits on the carbon monoxide abundance (or, of course, a positive detection) should allow us to probe further the processes that give rise to molecules of these early epochs.

3. Measurement of absorption by metastable He I could provide a useful diagnostic on the absorbing cloud temperature.

4. It may be profitable, given the intense radiation field inferred from the lack of H_2, to undertake an imaging study of the absorber in a narrow band of wavelengths centered in the Lyman-α absorption line.

In Paper III of this series we will expand the analysis presented here to study the conditions in the high column density, lower ionization cloud toward MC 1331+170 that exhibits C I absorption.

We have enjoyed conversations on these topics with Ray Weymann and Art Wolfe. This research was supported by grant AST 83-03766 from the National Science Foundation.

REFERENCES

Aaronson, M., Black, J. H., and McKee, C. F. 1974, *Ap. J. (Letters)*, **191**, L53.
Black, J. H., and Willner, S. P. 1984, *Ap. J.*, **279**, 673.
Chaffee, F. H., Jr., Foltz, C. B., and Black, J. H. 1986, *Soviet Astr. Letters*, in press (Paper I).
Coleman, G., Carswell, R. F., Strittmatter, P. A., Williams, R. E., Baldwin, J., Robinson, L. B., and Wampler, E. J. 1976, *Ap. J.*, **207**, 1.
Draine, B. T. 1978, *Ap. J. Suppl.*, **36**, 595.
Field, R. W., Benoist d'Azy, O., Lavollee, M., Lopez-Delgado, R., and Tramer, A. 1983, *J. Chem. Phys.*, **78**, 2838.
Foltz, C. B., Chaffee, F. H., Jr., and Weymann, R. J. 1986, *A.J.*, **92**, 247.
Jura, M. 1975, *Ap. J.*, **197**, 575; erratum, *Ap. J.*, **202**, 561.
Lambert, D. L. 1978, *M.N.R.A.S.*, **182**, 249.
Levshakov, S. A., Khersonskii, V. K., and Varshalovich, D. A. 1986, *Soviet Astr.*, in press.
Meyer, D. M., Chaffee, F. H., Jr., Black, J. H., Foltz, C. B., and York, D. G. 1986, *Ap. J. (Letters)*, **308**, L7.
Morton, D. C. 1975, *Ap. J.*, **197**, 85.
Morton, D. C., and Dinerstein, H. L. 1976, *Ap. J.*, **204**, 1.
Spitzer, L., Jr., and Jenkins, E. B. 1975, *Ann. Rev. Astr. Ap.*, **13**, 133.
Takahara, F., Sofue, Y., Nakai, N., Inoue, M., Tabara, H., and Kato, T. 1984, *Pub. Astr. Soc. Japan*, **36**, 387.
van Dishoeck, E. F. and Black, J. H. 1982, *Ap. J.*, **258**, 533.
———. 1986, *Ap. J. Suppl.*, **62**, 109.
Wannier, P. G., Penzias, A. A., and Jenkins, E. B. 1982, *Ap. J.*, **254**, 100.
Weisheit, J. C. 1974, *Ap. J.*, **190**, 735.
Wolfe, A. M., Turnshek, D. A., Smith, H. E., and Cohen, R. D. 1986, *Ap. J. Suppl.*, **61**, 249 (WTSC).
Yang, J., Schramm, D. N., Steigman, G., and Rood, R. T. 1979, *Ap. J.*, **227**, 697.
York, D. G. 1975, *Ap. J. (Letters)*, **196**, L103.

JOHN H. BLACK: Steward Observatory, University of Arizona, Tucson, AZ 85721

FREDERIC H. CHAFFEE, JR., and CRAIG B. FOLTZ: Multiple Mirror Telescope Observatory, University of Arizona, Tucson, AZ 85721